THE ASTRONOMICAL JOURNAL, 123:1847–1863, 2002 April

C IV AND OTHER METAL ABSORPTION LINE SYSTEMS IN 18 $z = 4$ QUASARS

TORU MISAWA,[1,2] DAVID TYTLER,[2,3,4] MASANORI IYE,[2,5] LISA J. STORRIE-LOMBARDI,[3,4,6]
NAO SUZUKI,[1,3] AND ARTHUR M. WOLFE[3,4]
Received 2001 November 13; accepted 2001 December 18

ABSTRACT

We present a modest survey of quasar metal line absorption systems at redshifts 2.3–4.5. Relatively high signal-to-noise ratio ($\sim$25 pixel^{-1}) spectra of 18 quasars at 2 Å FWHM resolution show many absorption systems with strong metal lines in the region redward of the Lyα emission lines. We conducted a systematic search and found 55 C IV doublets, 19 Si IV doublets, three Mg II doublets, and seven N V doublets. The present data alone hint that the number of C IV absorption doublets per unit redshift, $N(z)$, decreases with increasing redshift for $2.3 < z < 4.5$ but at only the 1–2 σ level, for either an Einstein–de Sitter model ($\Lambda = 0$) or a flat universe with $\Lambda = 0.7$. When we combine our sample with published data that extend to lower redshifts, we detect evolution at the 1–4 σ level, depending on the cosmological model and the strength of the C IV lines. There are fewer C IV systems per unit z with increasing z, and the systems with stronger C IV lines evolve much faster. At $z \simeq 2.4$, C IV with $W > 0.3$ Å are approximately 55% of all C IV systems with $W > 0.15$ Å, but by $z \simeq 4$ that percentage is less than 37%. Similar conclusions were reached by Sargent, Boksenberg, & Steidel and by Steidel, primarily at lower redshifts. However, we measure approximately twice the density of C IV systems at $2.3 < z < 3.8$ with $W > 0.15$ Å that was reported by Steidel. The probability that our sample and previous samples come from the same distribution is only $\sim$2%. But this could be a statistical accident because it is an a posteriori comparison. We believe that the systems that we report are real, and we have no other explanation for this difference. For Si IV absorption lines, there is a 1 σ hint of evolution with the same sense. In contrast, Lyα and Mg II systems are known to show evolution of the opposite sense with more absorbers at larger redshifts. The physical cause of this difference may be a mixture of ionization and chemical evolution effects.

Key words: galaxies: abundances — galaxies: evolution — quasars: absorption lines

1. INTRODUCTION

The absorption line properties of bright quasars at $z > 4$ have been investigated in detail for only a few objects because such observations require large telescopes. We obtained low-resolution (2 Å FWHM) spectra of a sample of 31 high-redshift quasars to find damped Lyα absorption (DLA) systems and to measure the cosmological density of baryons in these absorbers. As a secondary objective, we use these spectra to survey C IV absorption, which requires spectra covering the red side of Lyα emission and ideally extending to just beyond C IV emission. In total, we have useful spectra of the C IV region for 18 quasars, with a mean emission redshift of 3.9. The present study is not perfect in either sample size or spectral resolution but is sufficient to derive the general properties of the C IV absorption at these high redshifts.

The C IV doublet is well studied because it is usually the strongest among the metal lines, and these lines are often located at wavelengths redward of the Lyα forest. Young, Sargent, & Boksenberg (1982) presented the first major survey of C IV systems in 33 quasars and concluded that most arose in intervening gases. Foltz et al. (1986) obtained 1 Å spectra of 31 quasars at $z_{\rm em} \simeq 1.7$ and found that there is an excess of C IV absorbers with $z_{\rm abs} \simeq z_{\rm em}$. Sargent, Boksenberg, & Steidel (1988, hereafter SBS88) and Steidel (1990, hereafter S90) found that the number of C IV systems per unit redshift decreases with increasing z. It is still unclear whether this phenomenon is due to the continued production and mixing of carbon from the chemical evolution of stars or to changing ionization levels associated with the background UV flux. However, most workers accept the working hypothesis that the evolution of the number of C IV system is related to star formation in galaxies. The metal lines are thought to arise in metal absorption clouds in the outer regions of intervening galaxies. For Mg II and C IV absorption lines, there have been systematic investigations of the statistical properties of extended absorbing gas around galaxies, which suggest that galaxies are surrounded by chemically enriched gas that extends for at least $\sim$50 h^{-1} kpc for Mg II and $\sim$100 h^{-1} kpc for C IV (Bergeron & Boissé 1991; Chen, Lanzetta, & Webb 2001).

All but one of our 18 quasars have higher $z_{\rm em}$ than those studies in S90. But the $z_{\rm abs}$ coverage of our spectra is similar to that of past work, because many of our spectra do not extend to the C IV emission line of the quasars. In this paper, the primary goal is to improve the statistics of $N(z)$ following SBS88 and S90.

For Si IV absorption systems, no large statistical studied have been presented. Although our sample of 19 Si IV systems is small, we present statistics in this paper for the first time. The results are similar to those for C IV.

[1] Department of Astronomy, School of Science, University of Tokyo, 7-3-1 Hongo, Bunkyo-ku, Tokyo 113-0033 Japan; misawatr@cc.nao.ac.jp.
[2] National Astronomical Observatory, 2-21-1 Osawa, Mitaka, Tokyo 181-8588, Japan.
[3] Center for Astrophysics and Space Sciences, University of California, San Diego, MS 0424, La Jolla, CA 92093-0424.
[4] Visiting Astronomer, W. M. Keck Observatory, which is a joint facility of the University of California, the California Institute of Technology, and NASA.
[5] Department of Astronomical Science, The Graduate University for Advanced Stuides, 2-21-1 Osawa, Mitaka, Tokyo 181-8588, Japan.
[6] *SIRTF* Science Center, California Institute of Technology, MS 220-6, Pasadena, CA 91125.

In § 2 we present the outline of the observation and describe the identification of absorption lines. In § 3 we describe the characteristics of the individual absorption systems. We discuss the statistical analysis of C IV absorption systems for $2.3 < z_{abs} < 4.5$ and compare our results with previous work in § 4. The summary and discussion are in § 5.

2. DATA

2.1. *Keck LRIS Spectra*

Quasars were selected as a part of a survey for DLA systems. More details and low-resolution plots of spectra are given in Storrie-Lombardi & Wolfe (2000). The systems either contain either a known DLA candidate or have redshift $z_{em} \geq 3$ and $V \leq 20$, and all had no previously published equivalent data. We show later that this selection does not bias our search for C IV absorbers.

All observations used the Low Resolution Imaging Spectrometer (LRIS; Oke et al. 1995) on the Keck 1 telescope. The signal-to-noise ratios (S/N) of the resulting spectra are about 25 pixel^{-1}, and the resolution is about 2 Å (FWHM). Table 1 is the journal of observations of the 18 quasars. Column (1) gives the quasar coordinate identification, column (2) the emission redshift, column (3) the UT date of observation, columns (4) and (5) the V and R magnitudes, columns (6) and (7) the observed wavelength ranges, and column (8) the exposure time in seconds. All observations were obtained with a 0".7 slit. The spectra were wavelength-calibrated with a Th-Ar lamp, flat-fielded with a quartz lamp, and reduced using IRAF scripts. Arcs and flats were taken at the position of each observation to reduce the effects of fringing at the redder wavelengths.

2.2. *Identification of Absorption Lines*

At first, we looked at the spectra of our 18 quasars and marked troughs that looked like real absorption lines. We inspected the spectra of the sky emission lines to help identify and remove features that arose from poor sky subtraction. Absorption features that are at the wavelengths of sky emission or atmospheric absorption lines were rejected unless they were much stronger than expected from the atmosphere alone. After that, we identified each line with the candidate metal lines.

One of our main goals is to make a reasonably complete sample of C IV doublets. Table 2 lists all C IV lines that satisfy the following constraints:

1. Line strength: $W \geq 4\sigma(W)$ for C IV (λ1548) and $W \geq 2\sigma(W)$ for C IV (λ1551), where W is the equivalent width in angstroms.
2. Doublet ratio: $DR_{min} < DR < DR_{max}$, where $DR = W(1548)/W(1551)$.
3. Redshift difference: $|z(1548) - z(1550)| < 0.0015$.

The DR values were constrained to lie within the range 1.07–2.0, with allowance for line blending and measurement errors. The third criterion allows for the spectral resolution of our observation. These conditions are reasonable for C IV absorption lines. Table 2 also contains Si IV, Mg II, and N V doublets that satisfy equivalent criteria and singlet metal absorption lines with $W \geq 4\sigma(W)$ at the redshifts of these doublets.

Table 2 lists all lines that satisfy the criteria given above, but it excludes the lines that are apparently affected by sky emission lines. Column (1) is the line number; column (2) is the observed wavelength of absorption lines. Columns (3) and (4) give the observed and the rest-frame equivalent widths. If the line was identified as one or more of the metal lines, the metal line ascribed and its absorption redshift is presented in columns (5) and (6). If lines are in blends, the tabulated equivalent widths of each line is given in parentheses using all parts of the absorption line. This evaluation is correct only if the absorption line is not a blend of different ions. In Figure 1, we show the spectra. At the bottom of each spectrum, the 1 σ uncertainty is plotted. In the next section, we describe the characteristics of the individual systems.

3. RESULT OF IDENTIFICATIONS

3.1. *Discussion of Individual Spectra*

3.1.1. *BR 0019−1522* ($z_{em} = 4.528$)

$z_{abs} = 3.3720$.—This redshift is identified by only a weak C IV doublet.

$z_{abs} = 3.3936$.—Along with the strong C IV doublet, there is a moderately strong Fe II λ1608 line at this redshift.

$z_{abs} = 3.4370$.—This system, a known DLA, shows Si II λ1526, Fe II λ1608, and Al II λ1670.

$z_{abs} = 3.6097$.—Strong C IV doublet makes this a certain system. Fe II λ1608 line is also found for this redshift, but the line is certainly blended with other lines.

$z_{abs} = 3.7087$.—An unambiguous C IV doublet defines this redshift.

$z_{abs} = 3.7516$.—This redshift is identified by a moderately strong C IV doublet.

3.1.2. *SGP 0046−293* ($z_{em} = 4.014$)

$z_{abs} = 2.9950$.—This system is identified by a weak C IV doublet.

$z_{abs} = 3.0594$.—Along with a weak C IV doublet, there is a strong Si II λ1526 line.

$z_{abs} = 3.0719$.—The doublet ratio of the C IV doublet is unphysical. There may be two closely spaced C IV doublet in this system. The C I λ1656 line is also found at this redshift.

3.1.3. *SGP 0057−274* ($z_{em} = 3.52$)

$z_{abs} = 2.5422$, 2.5529.—This double C IV doublet is found near the peak of the Lyα emission line.

$z_{abs} = 2.6352$.—The strong C IV doublet makes this a certain system. Both the components of this doublet have W_{rest} larger than 0.6 Å.

3.1.4. *PSS 0059−0003* ($z_{em} = 4.16$)

$z_{abs} = 3.1036$.—Along with the C IV doublet, we see the Si II λ1526 line. There may be two closely spaced C IV doublets in this system.

$z_{abs} = 3.5191$.—C IV and Si IV doublets make this a certain system, but the redshift agreement between the Si IV doublet lines is not particularly good.

3.1.5. *PC 0104+0215* ($z_{em} = 4.171$)

$z_{abs} = 3.1822$.—We see a moderately strong C IV doublet and Si II λ1526 and Al II λ1670 lines.

TABLE 1
LRIS JOURNAL OF OBSERVATIONS

Quasar (1)	z_{em} (2)	Date (3)	V (mag) (4)	R (mag) (5)	λ_{min} (Å) (6)	λ_{max} (Å) (7)	Integration Time (s) (8)
BR 0019−1522........	4.528	1995 Sep 18		19.0	5200	6505	3300
					6400	7700	1200
					7800	9085	1500
SGP 0046−293........	4.014	1995 Sep 19	19.4		4705	6015	2400
					5900	7205	1200
SGP 0057−274........	3.52	1995 Sep 20		18.73	4370	5700	1500
					5595	6905	600
PSS 0059−0003.......	4.16	1995 Sep 19		19.5	4490	5810	2400
					5700	7010	1200
PC 0104 + 0215	4.171	1995 Sep 20	19.7		4705	6015	3600
					5850	7155	2400
BRI 0111−2819	4.30	1995 Sep 20		18.7	4705	6015	4300
		1995 Sep 20			6200	7505	1200
		1995 Sep 19			4485	5810	2400
		1995 Sep 19			5700	7010	1200
PC 0131 + 0120	3.792	1995 Sep 20		19.4	4990	6300	1500
					6200	7505	1200
Q0201 + 1120	3.61	1995 Sep 19	20.1		4990	6300	1800
		1995 Sep 19			5900	7205	1500
		1995 Sep 19			6900	8195	1200
PSS 0248 + 1802	4.43	1995 Sep 18		18.4	4490	5810	1700
					5700	7010	1200
					6900	8195	600
Q0249−222.............	3.20	1995 Sep 18	18.4		4485	5810	1200
					5700	7010	500
PC 0345 + 0130	3.638	1995 Sep 20	19.9		4485	5810	2400
		1995 Sep 19			5595	6905	1500
Q1500 + 0431	3.67	1995 Sep 20		18.01	4375	5700	1200
					5595	6905	600
PC 1548 + 4637	3.544	1995 Sep 20	19.2		4375	5700	2400
					5595	6900	600
PC 1640 + 4628	3.700	1995 Sep 19	19.5		4370	5690	1800
		1995 Sep 20			5595	6905	2100
PC 2047 + 0123	3.799	1995 Sep 18	19.7		4375	5700	5400
					5600	6905	1800
SGP 2050−359........	3.49	1995 Sep 19	18.3		4370	5700	1200
					5595	6905	600
BR 2237−0607........	4.558	1995 Sep 18		18.3	5900	7195	2400
					7100	8395	1200
PC 2331 + 0216	4.093	1995 Sep 19	20.0		4990	6300	2800
					6200	7505	1200

$z_{abs} = 3.7081$.—A certain Si IV doublet defines this system.

3.1.6. *BRI 0111−2819* ($z_{em} = 4.30$)

$z_{abs} = 1.3894$.—We see a strong Mg II doublet and the Mg I λ2852 line.

$z_{abs} = 3.1043$.—This DLA shows Fe II λ1608 and Al II λ1670 lines.

$z_{abs} = 3.1699$.—C IV doublet is found near the peak of the Lyα emission line. Although both components of this doublet have large equivalent widths, the C IV λ1551 line is certainly blended.

$z_{abs} = 3.8893$.—This redshift has a Si IV doublet and a C II λ1334 line. Despite the fact that the Si IV doublet ratio is unphysical, this system is certainly real.

3.1.7. *PC 0131+0120* ($z_{em} = 3.792$)

$z_{abs} = 2.9025$.—An unambiguous C IV doublet defines this redshift.

$z_{abs} = 3.0328$.—This system shows a moderately strong C IV doublet.

$z_{abs} = 3.2951$.—Another system defined by a weak C IV doublet.

$z_{abs} = 3.4205$, 3.4240—In addition to the double Si IV doublets, the C IV doublet is found in this redshift system.

3.1.8. *Q0201+1120* ($z_{em} = 3.61$)

$z_{abs} = 1.5732$.—Along with the relatively strong Mg II doublet, Fe II λ2344, Fe II λ2382, Fe II λ2586, Fe II λ2600, and Mg II λ2852 lines are found for this redshift.

TABLE 2

Absorption Lines

Line Number (1)	λ_{obs} (Å) (2)	W_{obs} (Å) (3)	W_{rest} (Å) (4)	ID (5)	z_{abs} (6)
BR 0019−1522 (z_{em} = 4.528)					
1	6768.7	0.74	0.17	C IV (λ1548)	3.3720
2	6773.9	3.46	0.78	Si II (λ1526)	3.4369
3	6780.0	0.41	0.09	C IV (λ1551)	3.3720
4	6799.1	1.47			
5	6802.1	1.48	0.34	C IV (λ1548)	3.3936
6	6813.5	0.74	0.17	C IV (λ1551)	3.3936
7	7065.0	0.72	0.16	Fe II (λ1608)	3.3924
8	7095.2	0.38			
9	7101.2	1.14			
10	7109.8	0.47			
11	7125.8	0.29			
12	7136.7	2.09	0.45	C IV (λ1548)	3.6097
			(0.47)	Fe II (λ1608)	3.4370
13	7148.4	1.43	0.31	C IV (λ1551)	3.6096
14	7289.9	0.65	0.14	C IV (λ1548)	3.7087
15	7302.0	0.38	0.08	C IV (λ1551)	3.7086
16	7356.4	1.34	0.28	C IV (λ1548)	3.7516
17	7369.7	0.87	0.18	C IV (λ1551)	3.7523
18	7413.3	3.30	(0.72)	Fe II (λ1608)	3.6090
			(0.69)	C I (λ1560)	3.7512
			(0.74)	Al II (λ1670)	3.4370
19	7548.0	0.51			
20	7567.5	0.40			
21	7848.0	1.05			
22	8512.2	0.77			
SGP 0046−293 (z_{em} = 4.014)					
1	6128.1	1.02			
2	6185.1	0.41	0.10	C IV (λ1548)	2.9950
3	6194.8	0.32	0.08	C IV (λ1551)	2.9947
4	6196.9	0.64	0.16	Si II (λ1526)	3.0590
5	6247.0	0.77			
6	6284.8	0.69	0.17	C IV (λ1548)	3.0594
7	6294.9	0.39	0.10	C IV (λ1551)	3.0592
8	6304.1	1.73	0.42	C IV (λ1548)	3.0719
9	6313.9	0.46	0.11	C IV (λ1551)	3.0715
10	6316.6	0.27			
11	6461.2	2.29			
12	6713.6	0.93			
13	6748.6	0.61	0.15	C I (λ1656)	3.0730
14	6781.6	0.53			
15	6800.5	0.39			
16	6823.8	1.46			
SGP 0057−274 (z_{em} = 3.52)					
1	5484.0	0.79	0.22	C IV (λ1548)	2.5422
2	5492.9	0.65	0.18	C IV (λ1551)	2.5420
3	5500.6	0.85	0.24	C IV (λ1548)	2.5529
4	5510.6	0.46	0.13	C IV (λ1551)	2.5535
5	5523.1	0.43			
6	5628.1	2.31	0.64	C IV (λ1548)	2.6353
7	5638.2	2.30	0.63	C IV (λ1551)	2.6357
8	5649.6	0.57			
9	5660.5	0.70			
10	5838.8	0.67			
PSS 0059−0003 (z_{em} = 4.16)					
1	6266.1	0.33	0.08	Si II (λ1526)	3.1043
2	6297.9	0.76	0.17	Si IV (λ1393)	3.5187
3	6332.7	1.22			
4	6339.9	0.59	0.13	Si IV (λ1402)	3.5196
5	6352.0	0.77	0.19	C IV (λ1548)	3.1028
6	6354.5	0.86	0.21	C IV (λ1548)	3.1045
7	6362.6	0.48	0.12	C IV (λ1551)	3.1028
8	6365.1	0.47	0.11	C IV (λ1551)	3.1045
9	6621.8	0.49			
10	6624.0	0.58			
11	6996.5	2.38	0.53	C IV (λ1548)	3.5191
12	7008.0	1.38	0.31	C IV (λ1551)	3.5190
PC 0104+0215 (z_{em} = 4.171)					
1	6385.9	0.88	0.21	Si II (λ1526)	3.1828
2	6474.9	2.06	0.49	C IV (λ1548)	3.1822
3	6485.8	1.30	0.31	C IV (λ1551)	3.1823
4	6561.9	2.46	0.52	Si IV (λ1393)	3.7081
5	6604.3	1.84	0.39	Si IV (λ1402)	3.7080
6	6689.6	0.56			
7	6825.6	1.09			
8	6842.5	0.77			
9	6936.9	0.97			
10	6989.1	1.36	0.33	Al II (λ1670)	3.1831
11	7006.2	0.56			
BRI 0111−2819 (z_{em} = 4.30)					
1	6455.8	3.29	0.79	C IV (λ1548)	3.1699
2	6461.6	3.56			
3	6465.5	2.27	0.54	C IV (λ1551)	3.1692
4	6471.4	1.05			
5	6481.1	5.45			
6	6515.6	0.75			
7	6525.3	3.36	0.69	C II (λ1334)	3.8896
8	6532.0	0.77			
9	6549.8	1.15			
10	6601.8	3.61	0.88	Fe II (λ1608)	3.1044
11	6625.4	0.44			
12	6681.5	3.56	1.49	Mg II (λ2796)	1.3894
13	6698.5	2.91	1.22	Mg II (λ2803)	1.3893
14	6750.7	0.54			
15	6814.5	3.50	(1.47)	Mg I (λ2852)	1.3887
			0.72	Si IV (λ1393)	3.8893
16	6857.3	5.27	(1.28)	Al II (λ1670)	3.1042
			1.08	Si IV (λ1402)	3.8884
PC 0131+0120 (z_{em} = 3.792)					
1	5903.3	0.18			
2	5908.4	0.42			
3	6032.4	0.87			
4	6041.8	1.83	0.47	C IV (λ1548)	2.9025
5	6051.0	1.54	0.39	C IV (λ1551)	2.9019
6	6056.3	0.37			
7	6060.4	0.34			
8	6161.1	0.76	0.17	Si IV (λ1393)	3.4205
9	6165.7	1.53	0.35	Si IV (λ1393)	3.4238
10	6201.1	0.40	0.09	Si IV (λ1402)	3.4206
11	6205.6	0.66	0.15	Si IV (λ1402)	3.4238
12	6223.9	0.48			
13	6243.6	1.67	0.41	C IV (λ1548)	3.0328
14	6254.1	0.78	0.19	C IV (λ1551)	3.0329
15	6563.5	0.35			
16	6573.9	0.33			
17	6649.7	0.90	0.21	C IV (λ1548)	3.2951
18	6660.7	0.69	0.16	C IV (λ1551)	3.2951
19	6849.2	3.62	0.82	C IV (λ1548)	3.4240

TABLE 2—*Continued*

Line Number (1)	λ_{obs} (Å) (2)	W_{obs} (Å) (3)	W_{rest} (Å) (4)	ID (5)	z_{abs} (6)
20............	6860.2	2.55	0.58	C IV (λ1551)	3.4237
21............	7035.6	0.39			
22............	7045.6	0.61			
Q0201+1120 (z_{em} = 3.61)					
1............	5666.6	0.74			
2............	5710.6	3.55	0.96	C IV (λ1548)	2.6886
			(0.81)	O I (λ1302)	3.3855
3............	5719.8	1.90	0.51	C IV (λ1551)	2.6884
			(0.43)	Si II (λ1304)	3.3851
4............	5851.5	2.65	0.63	Si IV (λ1393)	3.1984
			(0.60)	C II (λ1334)	3.3847
5............	5854.7	2.01			
6............	5879.6	0.74			
7............	5890.0	1.24	0.30	Si IV (λ1402)	3.1988
8............	5895.4	0.46			
9............	6032.6	0.76	0.30	Fe II (λ2344)	1.5734
10............	6086.9	1.41	0.32	Si IV (λ1393)	3.3673
11............	6111.7	1.50	(0.41)	C I (λ1656)	2.6886
			0.34	Si IV (λ1393)	3.3851
12............	6126.2	0.91	0.21	Si IV (λ1402)	3.3672
13............	6132.1	1.62	0.63	Fe II (λ2382)	1.5735
14............	6144.9	0.75			
15............	6152.0	0.71	0.16	Si IV (λ1402)	3.3856
16............	6253.9	1.03	0.25	C IV (λ1548)	3.0395
17............	6264.6	0.77	0.19	C IV (λ1551)	3.0397
18............	6656.6	0.88	0.34	Fe II (λ2586)	1.5734
19............	6663.9	0.44			
20............	6690.8	1.49	0.58	Fe II (λ2600)	1.5732
21............	6694.4	2.36	(0.58)	C I (λ1656)	3.0402
			(0.54)	Si II (λ1526)	3.3849
22............	6761.3	1.87	0.43	C IV (λ1548)	3.3672
23............	6772.2	1.35	0.31	C IV (λ1551)	3.3670
24............	6788.0	1.48	0.34	C IV (λ1548)	3.3845
25............	6799.7	1.31	0.30	C IV (λ1551)	3.3847
26............	7053.1	1.74	0.40	Fe II (λ1608)	3.3850
27............	7195.7	3.19	1.24	Mg II (λ2796)	1.5732
28............	7214.2	3.16	1.23	Mg II (λ2803)	1.5733
29............	7326.9	2.75	0.63	Al II (λ1670)	3.3853
30............	7341.9	1.21	0.47	Mg I (λ2852)	1.5734
31............	7717.8	1.26			
PSS 0248−1802 (z_{em} = 4.43)					
1............	6683.6	0.44	0.10	C IV (λ1548)	3.3170
2............	6694.6	0.24	0.06	C IV (λ1551)	3.3170
3............	6885.4	1.52	0.31	Si IV (λ1393)	3.9402
4............	6910.0	0.89			
5............	6929.4	1.08	0.22	Si IV (λ1402)	3.9398
6............	6974.0	0.26			
7............	7147.2	0.33			
8............	7185.4	0.80	0.17	C IV (λ1548)	3.6411
9............	7196.3	0.47	0.10	C IV (λ1551)	3.6405
10............	7626.6	3.93			
11............	7638.6	2.19			
12............	7648.0	2.94	0.60	C IV (λ1548)	3.9399
13............	7660.4	1.34	0.27	C IV (λ1551)	3.9397
Q0249−222 (z_{em} = 3.20)					
1............	5106.1	0.27			
2............	5112.3	1.25	(0.33)	C II (λ1334)	2.8308
			0.38	C IV (λ1548)	2.3021
3............	5118.0	0.63	0.17	Si IV (λ1393)	2.6721
4............	5121.4	0.61	0.18	C IV (λ1551)	2.3025

TABLE 2—*Continued*

Line Number (1)	λ_{obs} (Å) (2)	W_{obs} (Å) (3)	W_{rest} (Å) (4)	ID (5)	z_{abs} (6)
5............	5123.8	0.47			
6............	5151.4	0.36	0.10	Si IV (λ1402)	2.6723
			(0.11)	C I (λ1560)	2.3015
7............	5340.8	0.54			
8............	5389.4	0.45	0.13	C IV (λ1548)	2.4811
9............	5399.1	0.33	0.10	C IV (λ1551)	2.4816
10............	5493.9	0.26			
11............	5607.4	0.43	0.12	Si II (λ1526)	2.6729
12............	5686.4	1.13	0.31	C IV (λ1548)	2.6729
13............	5695.6	0.54	0.15	C IV (λ1551)	2.6728
14............	5711.7	0.22			
15............	5715.8	0.18			
16............	5718.2	0.17			
17............	5843.6	0.85	0.22	C IV (λ1548)	2.7745
18............	5850.2	0.78	0.20	Si II (λ1526)	2.8319
19............	5853.5	0.36	0.09	C IV (λ1551)	2.7746
20............	5932.7	0.60	0.16	C IV (λ1548)	2.8320
21............	5942.0	0.42	0.11	C IV (λ1551)	2.8316
22............	6025.1	0.43			
23............	6083.1	0.30			
24............	6136.9	0.54	0.15	Al II (λ1670)	2.6731
25............	6163.2	0.29			
26............	6351.2	2.45	0.64	C I (λ1656)	2.8331
27............	6357.0	1.61	0.39	C IV (λ1548)	3.1061
28............	6361.6	1.33			
29............	6367.4	0.84	0.20	C IV (λ1551)	3.1060
30............	6392.2	0.42			
31............	6402.4	0.96	0.25	Al II (λ1670)	2.8320
32............	6464.9	0.80	0.19	C IV (λ1548)	3.1758
33............	6475.5	0.54	0.13	C IV (λ1551)	3.1757
PC 0345+0130 (z_{em} = 3.638)					
1............	5654.7	0.82	0.22	C IV (λ1548)	2.6524
2............	5664.3	0.60	0.16	C IV (λ1551)	2.6526
3............	5685.2	1.00			
4............	5720.4	1.31			
5............	5734.2	0.36			
6............	5807.0	7.48	3.60	Mg II (λ2796)	1.0766
7............	5821.5	6.75	3.25	Mg II (λ2803)	1.0765
			(1.77)	Si II (λ1526)	2.8131
8............	5905.2	2.60	0.68	C IV (λ1548)	2.8142
9............	5913.8	1.20	0.32	C IV (λ1551)	2.8135
10............	5923.1	1.52	0.73	Mg I (λ2853)	1.0761
11............	6129.5	1.45	0.37	C IV (λ1548)	2.9591
12............	6139.5	0.63	0.16	C IV (λ1551)	2.9590
13............	6257.1	0.67			
14............	6440.0	0.32			
15............	6619.2	0.78	0.20	Al II (λ1670)	2.9617
16............	6636.5	3.01			
17............	6722.5	1.17			
18............	6726.1	1.21			
19............	6729.2	1.73			
20............	6745.3	4.68			
21............	6749.7	0.32			
Q1500+0431 (z_{em} = 3.67)					
1............	5680.6	1.41			
2............	5778.9	0.43			
3............	5890.1	2.37	0.56	Si IV (λ1393)	3.2261
4............	5927.9	1.99	0.47	Si IV (λ1402)	3.2259
5............	6177.9	1.69	0.42	C IV (λ1548)	2.9904
6............	6188.4	1.18	0.30	C IV (λ1551)	2.9905
7............	6419.2	0.53			

TABLE 2—*Continued*

Line Number (1)	λ_{obs} (Å) (2)	W_{obs} (Å) (3)	W_{rest} (Å) (4)	ID (5)	z_{abs} (6)
8.............	6542.8	3.26	0.77	C IV (λ1548)	3.2261
9.............	6553.7	2.34	0.55	C IV (λ1551)	3.2261
10...........	6701.0	0.70			
PC 1548+4637 (z_{em} = 3.544)					
1.............	5559.8	0.51			
2.............	5568.5	1.80			
3.............	5584.8	0.76			
4.............	5607.6	2.60	0.57	N V (λ1238)	3.5266
5.............	5614.3	4.61	1.02	N V (λ1238)	3.5320
6.............	5625.1	2.18	0.48	N V (λ1242)	3.5261
7.............	5632.2	4.54	1.00	N V (λ1242)	3.5318
PC 1640+4628 (z_{em} = 3.700)					
1.............	5817.1	3.62	0.77	N V (λ1238)	3.6957
2.............	5835.3	2.70	0.58	N V (λ1242)	3.6953
3.............	6543.8	1.79	0.38	Si IV (λ1393)	3.6951
4.............	6586.2	1.27	0.27	Si IV (λ1402)	3.6951
PC 2047+0123 (z_{em} = 3.799)					
1.............	5890.4	0.78	0.21	C IV (λ1548)	2.8047
2.............	5896.6	0.30			
3.............	5901.5	0.64	0.17	C IV (λ1551)	2.8055
4.............	5909.7	6.80	1.43	N V (λ1238)	3.7704
5.............	5917.5	1.89	0.40	N V (λ1238)	3.7767
			0.49	C IV (λ1548)	2.8222
6.............	5928.4	5.42	1.15	N V (λ1242)	3.7702
			1.42	C IV (λ1551)	2.8228
7.............	5936.4	1.35	0.28	N V (λ1242)	3.7766
			(0.35)	C I (λ1560)	2.8046
8.............	5964.5	2.00	0.42	N V (λ1238)	3.8147
			(0.52)	C I (λ1560)	2.8226
9.............	5984.1	1.41	0.29	N V (λ1242)	3.8150
10...........	6000.4	0.99	(0.27)	Fe II (λ1608)	2.7305
			(0.22)	C II (λ1334)	3.4963
11...........	6015.1	0.42			
12...........	6064.5	0.48			
13...........	6082.9	0.32			
14...........	6097.1	0.44			
15...........	6247.7	1.09			
16...........	6262.8	0.60			
17...........	6266.5	0.94	(0.20)	O I (λ1302)	3.8124
			0.21	Si IV (λ1393)	3.4961
18...........	6306.9	1.79	(0.38)	C II (λ1334)	3.7259
			0.40	Si IV (λ1402)	3.4960
			(0.47)	C I (λ1656)	2.8064
19...........	6347.0	0.82	0.20	C IV (λ1548)	3.0996
			(0.17)	C I (λ1328)	3.7764
20...........	6357.4	0.63	0.15	C IV (λ1551)	3.0995
21...........	6586.1	1.72	0.36	Si IV (λ1393)	3.7254
22...........	6589.3	0.65			
23...........	6628.6	1.27	0.27	Si IV (λ1402)	3.7254
24...........	6631.9	0.24			
25...........	6668.9	0.42			
26...........	6678.8	0.30			
27...........	6711.3	0.69	0.14	Si IV (λ1393)	3.8153
28...........	6754.8	0.56	0.12	Si IV (λ1402)	3.8153
SGP 2050−359 (z_{em} = 3.49)					
1.............	5462.1	1.33	0.33	C II (λ1334)	3.0929
2.............	5566.4	1.94	0.47	C II (λ1334)	3.1710
3.............	5596.1	0.83			
4.............	5704.6	1.32	0.32	Si IV (λ1393)	3.0930

TABLE 2—*Continued*

Line Number (1)	λ_{obs} (Å) (2)	W_{obs} (Å) (3)	W_{rest} (Å) (4)	ID (5)	z_{abs} (6)
5.............	5741.2	1.02	0.25	Si IV (λ1402)	3.0928
6.............	5813.5	1.75	0.42	Si IV (λ1393)	3.1711
7.............	5851.0	1.16	0.28	Si IV (λ1402)	3.1710
8.............	6089.0	0.85			
9.............	6248.8	0.66	0.16	Si II (λ1526)	3.0930
10...........	6336.2	2.03	0.50	C IV (λ1548)	3.0926
11...........	6346.8	1.23	0.30	C IV (λ1551)	3.0927
			(0.30)	Si II (λ1526)	3.1572
12...........	6359.8	0.21			
13...........	6368.4	0.47	0.11	Si II (λ1526)	3.1713
14...........	6384.0	0.40	0.10	C IV (λ1548)	3.1235
			(0.10)	C I (λ1560)	3.0915
15...........	6394.7	0.30	0.07	C IV (λ1551)	3.1236
16...........	6433.3	0.57	0.14	C IV (λ1548)	3.1554
			(0.14)	C I (λ1560)	3.1231
17...........	6444.3	0.35	0.09	C IV (λ1551)	3.1555
18...........	6457.4	1.75	0.42	C IV (λ1548)	3.1709
19...........	6468.2	1.16	0.28	C IV (λ1551)	3.1710
20...........	6662.5	0.39			
21...........	6665.7	0.36			
22...........	6801.5	0.70	0.16	C IV (λ1548)	3.3932
23...........	6813.7	0.52	0.12	C IV (λ1551)	3.3937
24...........	6816.9	0.15			
25...........	6838.7	0.97	0.24	Al II (λ1670)	3.0931
BR 2237−0607 (z_{em} = 4.558)					
1.............	6764.9	3.01	0.57	C I (λ1280)	4.2845
2.............	6849.2	0.29	0.05	C I (λ1277)	4.3625
3.............	7066.2	1.25			
4.............	7301.0	0.23			
5.............	7311.6	0.45	0.08	Si IV (λ1393)	4.2460
6.............	7335.2	0.32			
7.............	7341.8	0.11			
8.............	7347.9	0.43	0.09	C IV (λ1548)	3.7461
9.............	7358.9	0.35	0.07	Si IV (λ1402)	4.2460
			0.07	C IV (λ1551)	3.7453
10...........	7364.9	0.48	0.09	Si IV (λ1393)	4.2842
			(0.10)	Si II (λ1526)	3.8240
11...........	7378.4	0.17			
12...........	7387.9	0.27			
13...........	7412.9	0.29	0.06	Si IV (λ1402)	4.2845
14...........	7468.5	1.45	0.30	C IV (λ1548)	3.8240
			0.27	Si IV (λ1393)	4.3585
15...........	7471.7	1.36	0.25	Si IV (λ1393)	4.3608
16...........	7475.7	0.95			
17...........	7478.8	1.33	0.28	C IV (λ1551)	3.8226
18...........	7487.8	0.36			
19...........	7491.1	0.50			
20...........	7498.8	0.29			
21...........	7508.1	0.69	0.14	C IV (λ1548)	3.8496
22...........	7517.1	0.77	0.14	Si IV (λ1402)	4.3588
23...........	7519.8	0.66	0.12	Si IV (λ1402)	4.3607
			0.14	C IV (λ1551)	3.8491
24...........	7541.2	0.22			
25...........	7558.7	0.41			
26...........	7753.8	1.35	0.27	Si II (λ1526)	4.0788
27...........	7862.4	1.16	0.23	C IV (λ1548)	4.0784
			(0.24)	C I (λ1656)	3.7452
28...........	7875.5	0.63	0.12	C IV (λ1551)	4.0784
29...........	8096.0	0.53	0.10	C IV (λ1548)	4.2293
30...........	8109.5	0.55	0.11	C IV (λ1551)	4.2293
31...........	8121.3	0.55	0.10	C IV (λ1548)	4.2457
32...........	8135.5	0.35	0.07	C IV (λ1551)	4.2461
33...........	8169.4	0.64	0.13	Fe II (λ1608)	4.0790

TABLE 2—*Continued*

Line Number (1)	λ_{obs} (Å) (2)	W_{obs} (Å) (3)	W_{rest} (Å) (4)	ID (5)	z_{abs} (6)
34...........	8181.4	0.96	(0.18)	Si II (λ1526)	4.3589
			0.18	C IV (λ1548)	4.2845
35...........	8194.9	0.48	0.09	C IV (λ1551)	4.2844
36...........	8296.7	1.40	0.26	C IV (λ1548)	4.3590
37...........	8311.0	0.90	0.17	C IV (λ1551)	4.3593
38...........	8344.9	0.46			
39...........	8351.8	0.42			
PC 2331+0216 ($z_{em} = 4.093$)					
1.............	6192.9	0.86			
2.............	6275.4	1.31	0.26	N V (λ1238)	4.0656
3.............	6294.9	0.70	0.14	N V (λ1242)	4.0651
4.............	6302.6	0.66	0.14	Si II (λ1304)	3.8319
5.............	6318.8	0.27			
6.............	6323.3	0.16			
7.............	7038.8	0.72			
8.............	7433.9	0.95	0.20	C IV (λ1548)	3.8017
9.............	7446.0	0.73	0.15	C IV (λ1551)	3.8015
10...........	7480.5	0.73	0.15	C IV (λ1548)	3.8317
11...........	7492.9	0.52	0.11	C IV (λ1551)	3.8317

$z_{abs} = 2.6886$.—This system consists of a strong C IV doublet as well as the C I λ1656 line. Although the C I λ1656 line is certainly blended, the identification seems correct.

$z_{abs} = 3.0395$.—A C IV doublet and the C I λ1656 line are found for this redshift.

$z_{abs} = 3.1984$.—This redshift is identified by a Si IV doublet, but the equivalent width of both the lines in the doublet are doubtful because of blending.

$z_{abs} = 3.3672$.—Along with the C IV doublet, there is Si IV doublet at this redshift.

$z_{abs} = 3.3845$.—We find Si II λ1304, C II λ1334, Si II λ1526, Fe II λ1608, Al II λ1670, and O I λ1302 lines along with C IV and Si IV doublets. The identification of O I λ1302 line may be questioned because such low-ionization ions are usually associated with mostly neutral absorbers.

3.1.9. *PSS 0248+1802* ($z_{em} = 4.43$)

$z_{abs} = 3.3170$.—A certain C IV doublet defines this system.

$z_{abs} = 3.6411$.—This redshift is identified by a rather weak C IV doublet.

$z_{abs} = 3.9399$.—This system consists of a relatively weak C IV doublet, along with a very weak Si IV doublet.

3.1.10. *Q0249−222* ($z_{em} = 3.20$)

$z_{abs} = 2.3021$.—A C IV doublet is found near the peak of the Lyα emission line. The C I λ1560 line is also found, but it might be blended.

$z_{abs} = 2.4811$.—A rather weak C IV doublet defines this system.

$z_{abs} = 2.6729$.—We found both C IV and Si IV doublets in the spectrum and rather strong Si II λ1526 and rather weak Al II λ1670 lines, which make this system certain.

$z_{abs} = 2.7745$.—A moderately strong C IV doublet defines this system.

$z_{abs} = 2.8320$.—This is a DLA. Si II λ1526, C II λ1334, C I λ1656, Al II λ1670 lines and a weak C IV doublet are also found.

$z_{abs} = 3.1061$.—There is some evidence for a multicomponent structure in this C IV doublet. It is likely that more components would be found with higher spectral resolution.

$z_{abs} = 3.1758$.—The C IV doublet is found near the peak of the C IV emission line. The velocity separation from the emission redshift is smaller than 5000 km s^{-1}; therefore, this system may be affected by the background quasar.

3.1.11. *PC 0345+0130* ($z_{em} = 3.638$)

$z_{abs} = 1.0766$.—This low-redshift system is identified on the basis of a strong Mg II doublet and the Mg I λ2853 line. Two components of the Mg II doublet are so strong that they reach zero intensity in our spectrum.

$z_{abs} = 2.6525$.—The C IV doublet is found near the peak of the Lyα emission line.

$z_{abs} = 2.8142$.—Along with a C IV doublet, there is a Si II λ1526 line for this redshift. But the Si II line is rather doubtful because it is heavily blended.

$z_{abs} = 2.9591$.—This system has a rather weak C IV doublet and the Al II λ1670 line.

3.1.12. *Q1500+0431* ($z_{em} = 3.67$)

$z_{abs} = 2.9904$.—An unambiguous C IV doublet defines this redshift.

$z_{abs} = 3.2261$.—This system has a relatively a strong C IV doublet along with the Si IV doublet.

3.1.13. *PC 1548+4637* ($z_{em} = 3.544$)

$z_{abs} = 3.5266$, 3.5320.—It is possible to identify two closely spaced N V doublets in this system, which is near the emission redshift.

3.1.14. *PC 1640+4628* ($z_{em} = 3.700$)

$z_{abs} = 3.6951$.—Rather strong N V and Si IV doublets make this a certain system. This system is found in the vicinity of the background quasar.

3.1.15. *PC 2047+0123* ($z_{em} = 3.799$)

$z_{abs} = 2.8047$.—This system consists of the C I λ1560, C I λ1656, and C IV doublets. But this system may not be real, because some lines are very weak and blended.

$z_{abs} = 2.8222$.—This system consists of a C IV doublet and the C I λ1560 line. The C IV doublet ratio is unphysical since these lines are certainly blended.

$z_{abs} = 3.0996$.—This system is identified by a weak C IV doublet.

$z_{abs} = 3.4961$.—This system has a Si IV doublet and the C II λ1334 line. The Si IV lines are heavily blended with other lines; therefore, the doublet ratio of the Si IV doublet may not be correct.

$z_{abs} = 3.7254$.—In addition to a weak Si IV doublet, there is a C II λ1334 line at this redshift.

$z_{abs} = 3.7299$.—We found the Fe II λ1608 line in this DLA.

$z_{abs} = 3.7704$.—An unambiguous N V doublet defines this redshift.

$z_{abs} = 3.7767$.—This system is identified by a moderately strong N V doublet along with a C I λ1328 line. But the C I identification could be wrong.

$z_{abs} = 3.8153$.—This system consists of rather weak Si IV and N V doublets at a redshift higher than the background quasar. This system is thought to be associated with the

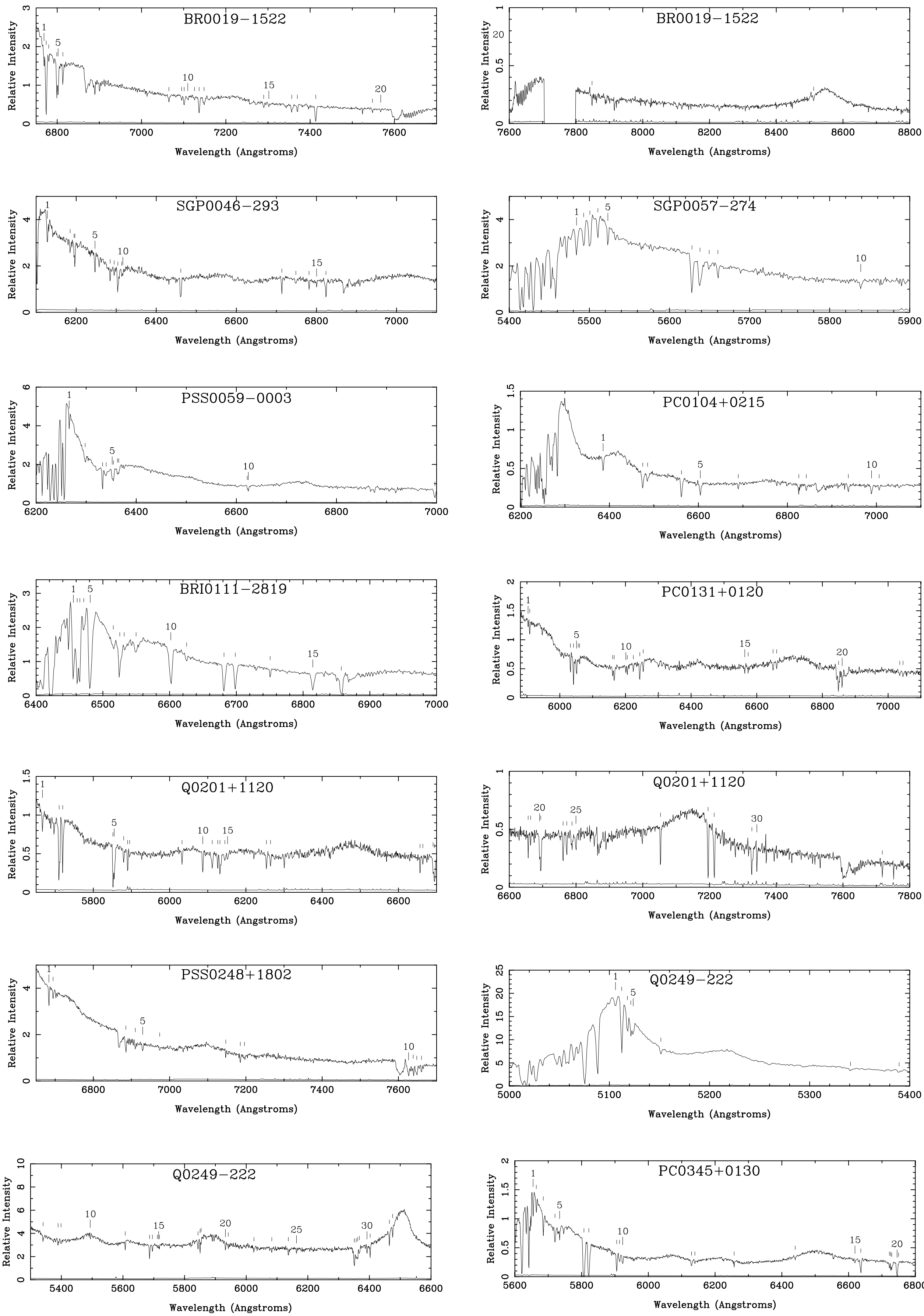

FIG. 1.—LRIS spectra of 18 quasars. Numbers above the absorption lines refer to Table 2.

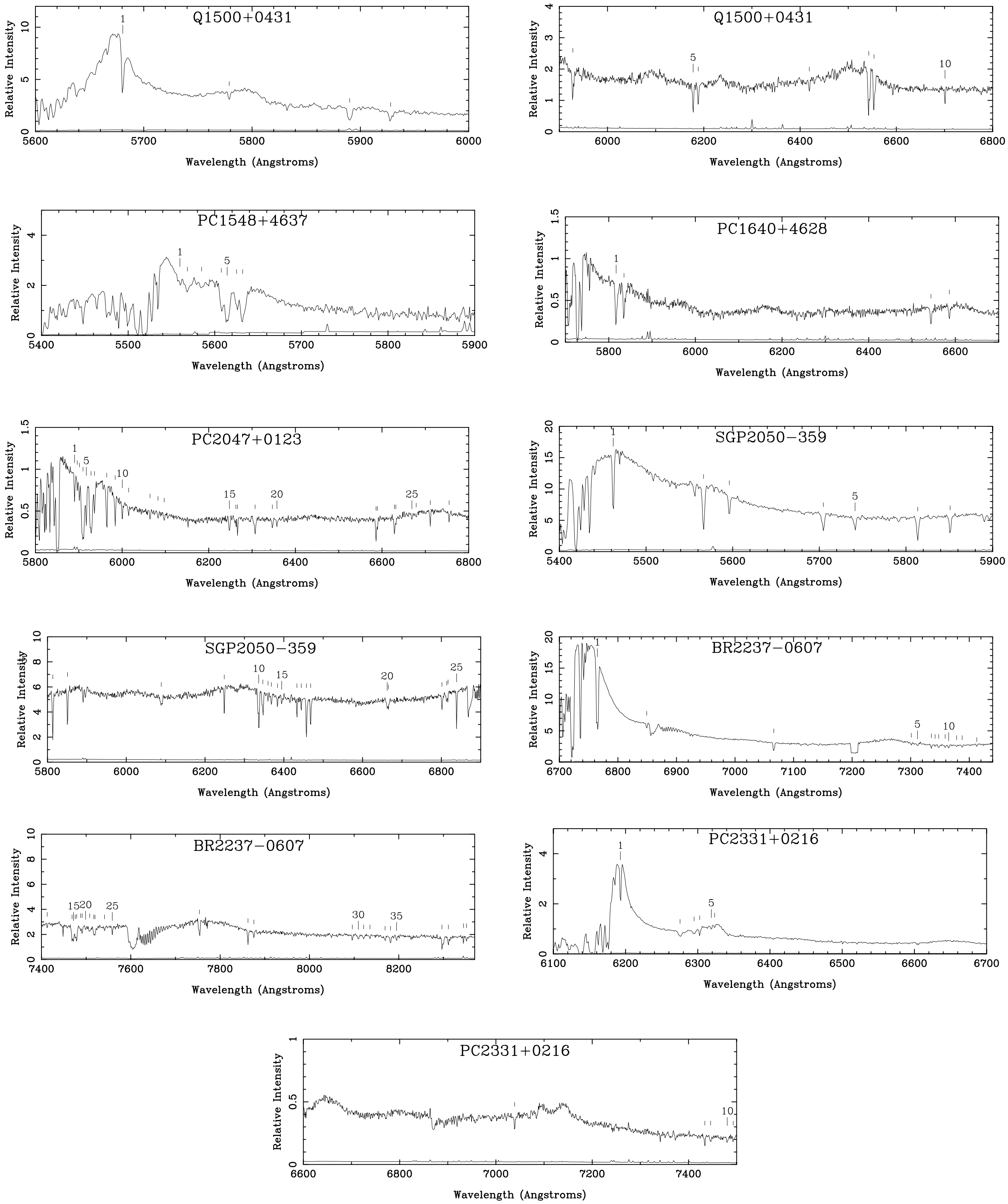

FIG. 1.—*Continued*

quasar itself. We also find line at this redshift which could be O I λ1302.

3.1.16. *SGP 2050−359* ($z_{\rm em} = 3.49$)

$z_{\rm abs} = 3.0926$.—This is a redshift system with many absorption lines. C IV and Si IV doublets are identified, along with the C II λ1334, Si II λ1526, C I λ1560, and Al II λ1670 lines. Although only one C IV doublet has been identified, it is likely that more components would be found with higher spectral resolution.

$z_{\rm abs} = 3.1235$.—This is a redshift system with a weak C IV doublet and the C I λ1560 line.

$z_{\rm abs} = 3.1554$.—A weak C IV doublet and the Si II λ1526 line define this system.

$z_{\rm abs} = 3.1709$.—This redshift system is identified by C IV and Si IV doublets as well as C II λ1334 and Si II λ1526 lines. The redshift agreement among the components is acceptable.

$z_{abs} = 3.3932$.—This system is identified by only a weak C IV doublet.

3.1.17. *BR 2237−0607* ($z_{em} = 4.558$)

$z_{abs} = 3.7461$.—Very weak C IV doublet defines this system along with the C I λ1656 line.

$z_{abs} = 3.8240$.—The redshift agreement between the two lines of the C IV doublet is not particularly good because of a multicomponent structure around this C IV doublet. It is likely that more components would be found with higher spectral resolution.

$z_{abs} = 3.8496$.—C IV doublet defines this system. But there is a high probability that this system is not real, because the two lines of this C IV doublet are heavily blended.

$z_{abs} = 4.0784$.—This DLA shows a C IV doublet and the Fe II λ1608 and Si II λ1526 lines.

$z_{abs} = 4.2293$, 4.2457.—It is possible to identify two closely spaced weak C IV doublets for this system. The velocity separation between these two doublets is less than 1000 km s^{-1}.

$z_{abs} = 4.2460$.—This system is identified by a weak Si IV doublet.

$z_{abs} = 4.2845$.—While the equivalent widths of the C IV and Si IV doublets are very small, the existence of a moderately strong C I λ1280 line adds credence to the identification of this system.

$z_{abs} = 4.3585$, 4.3608.—There is a multicomponent structure in this weak Si IV doublet. It is likely that more components would be found with higher spectral resolution. In addition to a pair of Si IV doublets, there are Si II λ1526 and C I λ1277 lines and a C IV doublet at this redshift.

3.1.18. *PC 2331+0216* ($z_{em} = 4.093$)

$z_{abs} = 3.8017$.—This redshift system has a rather weak C IV doublet.

$z_{abs} = 3.8317$.—A C IV doublet and the Si II λ1304 line make this a certain system.

$z_{abs} = 4.0656$.—This system is identified based on a rather shallow but very wide N V doublet. There is a possibility of multicomponent structure in this system. The velocity separation of this N V system from the emission redshift is very small.

3.2. *Discussion of the Metal Absorption Line Systems*

We identified many metal lines toward each of the 18 quasars. Since C IV, Si IV, Mg II, and N V lines are doublets, they are easy to identify. We found three Mg II, seven N V, 19 Si IV doublets, as well as 55 C IV doublets. We also found 63 singlet metal lines at the redshifts of these doublets. In a few systems, we identify low ionized absorption line such as C I and O I, which we consider as tentative, because such lines are rarely seen except in DLAs.

DLAs were already known in four of the quasars prior to the present observations with LRIS, but these did not bias the sample to include excess C IV lines. In three of the four cases, we found metal lines at the candidate redshifts, and in only two cases, $z = 2.8320$ in Q0249−222 and $z = 4.0784$ in BR 2237−0607, C IV systems were found at the DLA candidate redshifts. These two quasars would have been observed whether or not DLA candidates were known, because they were amongst the brightest known at high redshift.

4. C IV STATISTICAL ANALYSIS

4.1. *Statistical Samples*

SBS88 and S90 have previously shown that the number of C IV systems per unit z drops with rising z. In particular, they noted a very low density of C IV systems in their highest redshift bin, at 3.0–3.7. Our new spectra are well suited for checking this.

Before starting the statistical analysis, we must prepare homogeneous samples of C IV absorption systems that can be compared directly with those used in the earlier papers. The minimum observed-frame equivalent width (W_{min}) that we can detect depends on the S/N per pixel, following Young et al. (1979) and Tytler et al. (1987), and correcting an error in equation (5) of the latter,

$$U = \frac{W_{min} N_C}{\sigma(W_{min} N_C)} = \frac{W_{min}(S/N)}{(M_L^2 M_C^{-1} + M_L - W_{min})^{1/2}} , \quad (1)$$

where M_L and M_C are the numbers of pixels over which the equivalent width and the continuum level (N_C) are decided. When we set the $U \simeq W/\sigma(W) = 4$, the probability of obtaining a single bogus absorption line with $W > W_{min}$ is about 6% per spectrum, and equation (1) can be solved as follows:

$$W_{min} = (S/N)^{-2}\{[64 + 16(S/N)^2 \times (M_L + M_L^2/M_C)]^{1/2} - 8\} \times \Delta\lambda\ (\text{Å}) , \quad (2)$$

where $\Delta\lambda$ is the wavelength range per pixel in angstroms. We use equation (2) and the S/N in our spectra to find wavelength ranges in which the absorption lines with $W \geq W_{min}$ could be detected reliably with contamination less than 6% per spectrum when $W > W_{min}$.

In Table 3 we list the range of redshifts over which we could see C IV lines with rest-frame equivalent widths, $W_{rest}[= W_{min}/(1+z)]$, larger than 0.60 Å (which we later use for a sample which we call M60), 0.30 Å (M30), and 0.15 Å (M15). These redshift ranges depend on the S/N of the spectra. When we calculate the number density of C IV systems, we exclude absorbers that lie within $v = 5000$ km s^{-1} of the quasar z_{em}, following past work. Quasars have a strong influence on the ionization state of such gases. The z_{max} values that are limited by this effect are marked in Table 3. We also combine C IV absorption components that lie within 1000 km s^{-1} of each other to give single redshifts, and we evaluate just one DR using total equivalent widths following SBS88. This method is based on the possibility that clustered components are not physically independent and that the number of components seen is sensitive to the spectrum quality. Combined systems, so-called Poisson samples, are listed in Table 4. In columns (3) and (4), we listed the equivalent width of each C IV line, and the doublet ratio is presented in column (5). The system identification rules from § 2 gave 51 C IV systems in 16 out of our 18 quasars. In Table 4, we also added four C IV doublets that do not meet all the criterions described in § 2, because these doublets have sufficiently strong equivalent width or other accompanied metal lines at the same redshifts, and they are probably real absorption systems. In total, we found 55 C IV

TABLE 3
C IV REDSHIFT RANGE

		M60		M30		M15	
QUASAR (1)	z_{em} (2)	z_{min} (3)	z_{max} (4)	z_{min} (5)	z_{max} (6)	z_{min} (7)	z_{max} (8)
BR 0019−1522	4.528	3.335	4.520[a]	3.335	4.520[a]	3.335	4.520[a]
SGP 0046−293	4.014	2.953	3.654	2.953	3.654	2.953	3.654
SGP 0057−274	3.52	2.555	3.461[a]	2.555	3.461[a]	2.555	2.683
PSS 0059−0003	4.16	3.044	3.527	3.044	3.527	3.044	3.527
PC 0104+0215	4.171	3.069	3.623	3.069	3.623	3.069	3.623
BRI 0111−2819	4.30	3.166	3.528	3.166	3.528	3.166	3.528
PC 0131+0120	3.792	2.776	3.787[a]	2.776	3.787[a]	2.776	3.044
						3.270	3.396
						3.720	3.787[a]
Q0201+1120	3.61	2.643	3.617[a]	2.643	3.617[a]	2.643	2.781
						3.488	3.617[a]
PSS 0248+1802	4.43	3.262	4.295	3.262	4.295	3.262	4.005
Q0249−222	3.20	2.300	3.203[a]	2.300	3.203[a]	2.300	3.203[a]
PC 0345+0130	3.638	2.651	3.461	2.651	3.461	2.651	2.801
						3.136	3.322
Q1500+0431	3.67	2.667	3.461	2.667	3.461	2.667	2.759
PC 1548+4637	3.544	2.581	3.457	2.581	2.682	2.581	2.612
PC 1640+4628	3.700	2.713	3.460	2.713	3.460	...	...
PC 2047+0123	3.799	2.784	3.461	2.784	3.461	2.784	2.867
						3.264	3.433
SGP 2050−359	3.49	2.530	3.461[a]	2.530	3.461[a]	2.530	3.461[a]
BR 2237−0607	4.558	3.358	4.423	3.358	4.423	3.358	4.423
PC 2331+0216	4.093	3.000	3.843	3.000	3.843	3.000	3.843

[a] This redshift is within 5000 km s^{-1} of the z_{em}.

systems in the redshift range $2.3 \leq z \leq 4.5$, two of which we ignore because they are at $z < z_{min}$, leaving 53 systems. Figure 2 shows the redshift distribution of these 53 C IV absorption systems, which we denote sample M0. The solid histogram represents the number of C IV systems as a function of redshift. The dotted histogram is the number of quasars in which a C IV absorption redshift could have been detected. Note that this figure does not represent the unbiased distribution of C IV systems, because it includes the four additional systems, and systems with $W_{rest} < 0.15$ Å.

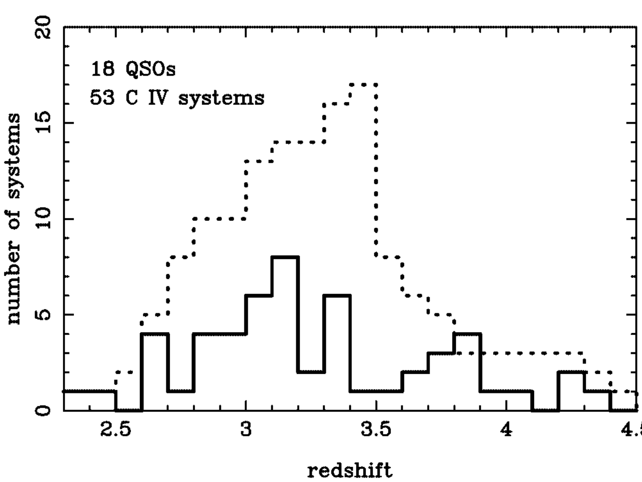

FIG. 2.—Solid histogram represents the number of absorption systems in sample M0 as a function of redshift. The dotted histogram is the number of quasars in which absorption lines could have been detected.

To define unbiased samples for statistical analyses, in Table 5 we classified C IV absorption systems into one or more of the four samples according to their W_{rest}. We reject the two systems with $z < z_{min}$ and the four systems that are certain but violated a rule from § 2. If both the lines in the doublet have W_{rest} larger than one of the three limits, 0.15, 0.3, and 0.6 Å, they are assigned to samples M15, M30, and M60, respectively. We find 29 systems in sample M15, 14 in sample M30, and only one in sample M60, as summarized in Table 5. Column (1) is the criteria of each sample. The mean redshift of the observed z_{abs} and weighted mean redshift of the sample ranges in Table 3 are presented in columns (4) and (5), respectively. Mean density of C IV absorption systems is presented in columns (6). These unbiased samples are used for the statistical analysis in the next section.

4.2. *Evolution of the* C IV *Systems*

We can fit the evolution of the number density of systems with redshift, $N(z)$, in the comoving volume, where

$$N(z) = N_0(1+z)(1+2q_0z)^{-1/2} \sim N_0(1+z)^{\gamma} \quad (3)$$

is the number of absorption systems per unit redshift at redshift z. If absorption systems have constant proper size and comoving volume, their N_0 does not change with redshift, and $\gamma = 1$ for the case $q_0 = 0$ and $\gamma = 0.5$ for the case $q_0 = 0.5$ in cosmological models with zero cosmological constant.

We studied the distribution of C IV lines using this method. Figures 3 and 4 show the arbitrarily binned number of C IV systems per unit z for the sample M15 and M30. Following equation (3), we evaluate indices of each sample.

TABLE 4
C IV ABSORPTION SYSTEMS

Quasar (1)	z_{abs} (2)	$W_{rest}(1548)$ (Å) (3)	$W_{rest}(1550)$ (Å) (4)	DR (5)	Sample (6)	Note (7)
BR 0019−1522........	3.3720	0.17	0.09	1.79	...	
	3.3936	0.34	0.17	1.99	M15	
	3.6097	0.45	0.31	1.46	M15, M30	
	3.7087	0.14	0.08	1.73	...	
	3.7516	0.28	0.18	1.55	M15	
SGP 0046−293........	2.9950	0.10	0.08	1.26	...	
	3.0594	0.17	0.10	1.75	...	
	3.0719	0.42	0.11	3.76	...	a
SGP 0057−274........	2.5422	0.22	0.18	1.23	...	b
	2.5529	0.24	0.13	1.85	...	b
	2.6352	0.64	0.63	1.01	M15, M30, M60	
PSS 0059−0003.......	3.1036	0.40	0.23	1.74	M15	c
	3.5191	0.53	0.31	1.72	M15, M30	
PC 0104+0215	3.1822	0.49	0.31	1.58	M15, M30	
BRI 0111−2819	3.1699	0.79	0.54	1.45	M15, M30	
PC 0131+0120	2.9025	0.47	0.39	1.19	M15, M30	
	3.0328	0.41	0.19	2.13	M15	
	3.2951	0.21	0.16	1.29	M15	
	3.4240	0.82	0.58	1.42	M15, M30	
Q0201+1120	2.6886	0.96	0.51	1.87	M15, M30	
	3.0395	0.25	0.19	1.34	...	
	3.3672	0.43	0.31	1.39	M15, M30	
	3.3845	0.34	0.30	1.13	M15, M30	
PSS 0248+1802	3.3170	0.10	0.06	1.81	...	
	3.6411	0.17	0.10	1.71	...	
	3.9399	0.60	0.27	2.20	M15	
Q0249−222............	2.3021	0.38	0.18	2.06	M15	
	2.4811	0.13	0.10	1.35	...	
	2.6729	0.31	0.15	2.11	M15	
	2.7745	0.22	0.09	2.38	...	
	2.8320	0.16	0.11	1.44	...	
	3.1061	0.39	0.20	1.91	M15	
	3.1758	0.19	0.13	1.49	...	d
PC 0345+0130	2.6525	0.22	0.16	1.36	M15	
	2.8142	0.68	0.32	2.16	M15, M30	
	2.9591	0.37	0.16	2.28	...	
Q1500+0431	2.9904	0.42	0.30	1.43	M15, M30	
	3.2261	0.77	0.55	1.39	M15, M30	
PC 1548+4637						
PC 1640+4628						
PC 2047+0123	2.8047	0.21	0.17	1.21	M15	
	2.8222	0.49	1.42	0.35	...	a
	3.0996	0.20	0.15	1.30	...	
SGP 2050−359........	3.0926	0.50	0.30	1.65	M15, M30	
	3.1235	0.10	0.07	1.35	...	
	3.1554	0.14	0.09	1.62	...	
	3.1709	0.42	0.28	1.51	M15	
	3.3932	0.16	0.12	1.34	...	
BR 2237−0607........	3.7461	0.09	0.07	1.25	...	
	3.8240	0.30	0.28	1.09	...	e
	3.8496	0.14	0.14	1.05	...	
	4.0784	0.23	0.12	1.85	...	
	4.2380	0.21	0.17	1.20	M15	c
	4.2845	0.18	0.09	1.99	...	
	4.3590	0.26	0.17	1.55	M15	
PC 2331+0216	3.8017	0.20	0.15	1.31	M15	
	3.8317	0.15	0.11	1.42	...	

[a] Doublet ratio is not appropriate, but other metal lines are found at the same redshift
[b] Redshift of absorber is smaller than z_{min} or bigger than z_{max}.
[c] Two absorbers are combined because they lie within 1000 km s^{-1} of each other.
[d] Absorber lies within 5000 km s^{-1} of the quasar z_{em}.
[e] $|z(1548) - z(1551)| > 0.0015$, but other metal lines are found at the same redshift.

TABLE 5
DENSITY OF C IV SYSTEMS

Criteria (1)	Sample (2)	Systems (3)	$\langle z_{abs}\rangle$[a] (4)	$\bar{z}$[b] (5)	$\overline{N}$[c] (6)	γ (7)	$\sigma(\gamma)$ (8)	G (9)	$\sigma(G)$ (10)
All included..........................	M0	53	...	...	...	−0.98	1.52	−1.58	1.56
$W_0 > 0.15,\ \beta c > 5000$.........	M15	29	3.229	3.360	$3.11^{+0.69}_{-0.57}$	−1.88	1.91	−2.45	2.05
$W_0 > 0.30,\ \beta c > 5000$.........	M30	14	3.143	3.306	$0.99^{+0.34}_{-0.26}$	−4.84	3.13	−5.38	3.13
$W_0 > 0.60,\ \beta c > 5000$.........	M60	1	2.635	3.295	$0.07^{+0.16}_{-0.06}$	...	...	...	...
$W_0 > 0.15,\ \beta c > 5000$[d]	EM15	136	2.372	2.457	$2.35^{+0.22}_{-0.20}$	−0.58	0.46	−1.18	0.47
$W_0 > 0.30,\ \beta c > 5000$[d]	EM30	72[e]	2.208	2.516	$1.15^{+0.15}_{-0.13}$	−2.20	0.72	−2.81	0.72

[a] Mean redshift of observed z_{abs}.
[b] Weighted mean redshift of the sample ranges in Table 3, following Tytler et al. 1987.
[c] Mean number of systems per unit redshift, at redshift $\bar{z}$.
[d] Includes data from SBS88 and S90.
[e] Excluding data from Young et al. 1982 and Foltz et al. 1986, which are included in equivalent samples of SBS88 and S90.

They are presented in Table 5. A trend of decreasing $N(z)$ with increasing z is hinted for all the samples, but in each case γ is within 1 or 1.5 σ of zero.

We also evaluated the number densities of C IV absorption systems per unit redshift, $\overline{N}$. The results are presented in Table 5. Mean redshift of M15, $z \sim 3.229$, is higher than those of M30 and M60, $z \sim 3.143$ and 2.635, while weighted mean redshifts of the sample ranges, $\bar{z}$, are almost same. This hints that systems with larger equivalent width are more prevalent at lower redshift even though there is only one system in M60. We also found that the number density of M15 is much higher than those of the other samples. These results are consistent with previous work. The only point that did not match past work, for no known reason, is that the number density of C IV systems in our sample M15 ($W_{rest} > 0.15$ Å) is about twice that of the similar sample in S90. A χ^2-test has been performed to compare our data and the previous data, which leads to the result that there is a 2% chance that the two samples were drawn from the same parent distribution. Both of the C IV doublet lines in previous work must have equivalent widths greater than $5\sigma(W)$, while in our samples C IV (λ1548) and C IV (λ1551) are accepted with $W \geq 4\sigma(W)$ and $W \geq 2\sigma(W)$, respectively. The effect of the difference between $5\sigma(W)$ and $4\sigma(W)$ is almost negligible, and all but one of the C IV systems in M15 has $W(1551)$ greater than $5\sigma(W)$. The larger density of systems in our sample appears to be real. The difference of number density is probably a statistical accident, because a 2% chance occurrence is common for such a posteriori statistics.

Here we show the form of $N(z)$ expected in a universe with a cosmological constant (Tytler 1981):

$$N(z) = cH_0^{-1}\phi(z)\Sigma(z)(1+z)^2 H_0/H(z)\ , \tag{4}$$

where

$$H(z)/H_0 = \sqrt{\Omega_0(1+z)^3 + \Omega_k(1+z)^2 + \Omega_\Lambda}\ , \tag{5}$$

and Ω_0 is the matter density, Ω_k is the curvature term, and Ω_Λ is the contribution of the cosmological constant. If absorbers have constant comoving density $\phi(z)$, and constant proper size $\Sigma(z)$, then we say they do not evolve, and we can set

$$N_0 = N(z=0) = cH_0^{-1}\phi(0)\Sigma(0). \tag{6}$$

On Figures 3 and 4 we plot $N(z) = N_0(1+z)^{2+G}H_0/H(z)$ for $\Omega_0 = 0.3$, $\Omega_\Lambda = 0.7$, and $\Omega_k = 1 - \Omega_0 - \Omega_\Lambda = 0$ with the

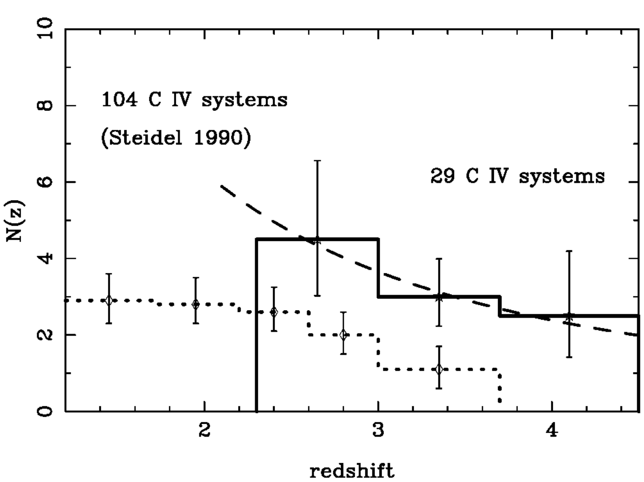

FIG. 3.—Distribution of the number of C IV absorption systems per unit redshift in arbitrarily bins as a function of z for sample M15. Data from the equivalent S90 sample are shown as the dotted histogram. The dashed curve is the maximum likelihood estimate of $G = -2.45$ from eq. (7).

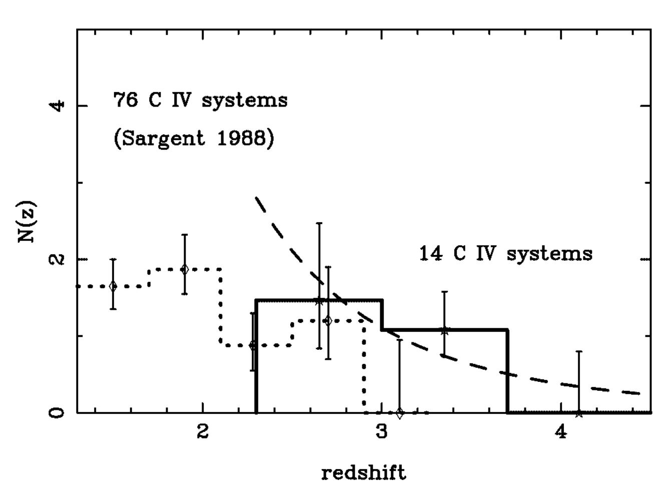

FIG. 4.—Same as Fig. 3, but for absorption systems in sample M30. Data from the equivalent SBS88 sample are shown as the dotted histogram. The dashed curve is the maximum likelihood estimate of $G = -5.38$ from eq. (7).

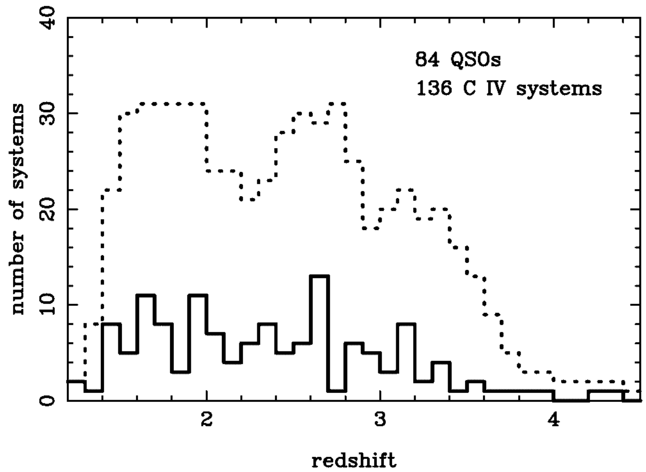

FIG. 5.—Same as Fig. 2, but for sample EM15, which includes data from SBS88 and S90.

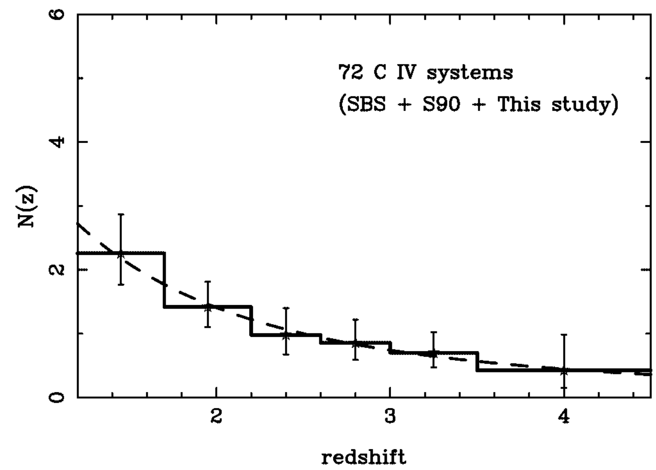

FIG. 7.—Same as Fig. 3, but for sample EM30. The dashed curve is the result of a maximum likelihood estimation for eq. (7) with $G = -2.81$.

free parameter, G, where

$$N(z) = N_0 \frac{(1+z)^{2+G}}{\sqrt{0.3(1+z)^3 + 0.7}} . \quad (7)$$

If N_0 does not change with redshift, $G = 0$. The evaluated indices for M15 and M30 are presented in Table 5, and they are all negative values, 1–2 σ away from the $G = 0$ no evolution case.

We have combined our M15 and M30 samples with their equivalents from SBS88 and S90 to form new samples of 136 redshifts for $W_{\rm min} \geq 0.15$ Å (EM15) and 72 redshifts for $W_{\rm min} \geq 0.30$ Å (EM30) found in the spectra of 84 quasars. Figure 5 shows the redshift distribution of combined sample EM15. We carry out the same statistical analyses for these new samples and fit the number density evolution in the two aforementioned models. The results are shown in Figures 6 and 7 for sample EM15 and EM30, respectively. The evolution indices are presented in Table 5. Sample EM15 shows little evolution, which is because at higher z our high $N(z)$ sample cancels out the lower $N(z)$ of SBS88 and S90. The γ index is 1 σ from zero, but G is 2 σ from zero—a significant detection of evolution if $\Omega_\Lambda = 0.7$, $\Omega_0 = 0.3$. On the other hand, the sample EM30 now clearly evolves, and comparison of the two samples shows that stronger systems are more prevalent at lower redshifts.

For Si IV absorption lines, we also attempted the same statistical analysis and got the same decreasing trend. The redshift ranges and Poisson samples of Si IV lines are summarized in Tables 6 and 7. Figure 8 shows the redshift distribution of these Si IV absorption systems. The results of the statistical analysis are presented in Figure 9 and Table 8. This is the first study of the evolution of number density of Si IV absorption lines. Almost all of these doublets are found at the redshift of C IV doublets. Again we see a hint (1 σ) of a decrease of $N(z)$ with increasing z.

We also found other metal absorption lines such as Mg II and N V. The three low-z Mg II doublets were all accompanied by the neutral magnesium line Mg I λ2852. These absorbers could have a lot of neutral gas, like DLAs. On the other hand, several quasars show strong N V systems, some with components, at redshift similar to their emission redshift. These N V absorbers could be highly ionized by UV flux from background quasars.

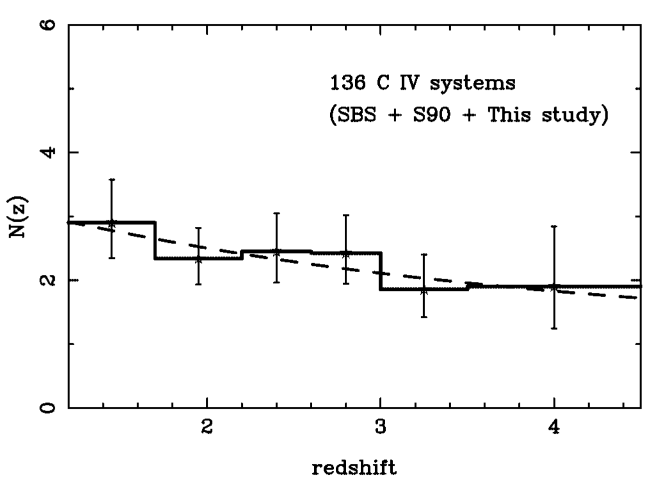

FIG. 6.—Same as Fig. 3, but for sample EM15. The dashed curve is the result of a maximum likelihood estimation for eq. (7) with $G = -1.18$.

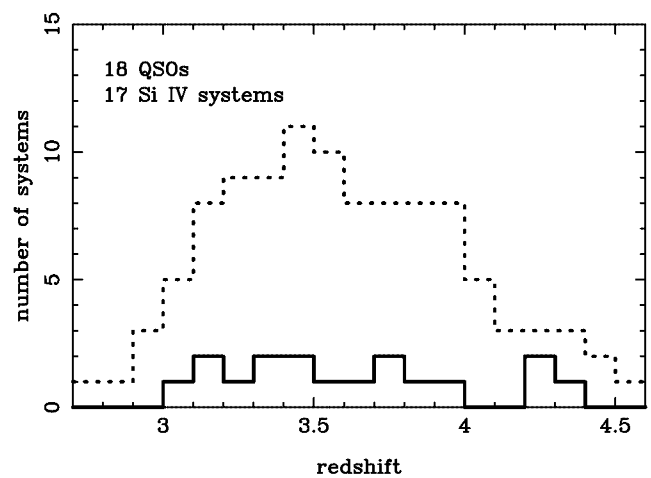

FIG. 8.—Same as Fig. 2, but for sample M0 of Si IV systems. We include all Si IV systems at $2.7 < z < 4.6$ but one system at $z \sim 2.67$.

TABLE 6

Si IV Redshift Range

Quasar (1)	z_{em} (2)	M60 z_{min} (3)	M60 z_{max} (4)	M30 z_{min} (5)	M30 z_{max} (6)	M15 z_{min} (7)	M15 z_{max} (8)
BR 0019−1522.....	4.528	3.814	4.528[a]	3.814	4.528[a]	3.814	4.528[a]
SGP 0046−293.....	4.014	3.390	4.014[a]	3.390	4.014[a]	3.390	4.014[a]
SGP 0057−274.....	3.52	2.948	3.520[a]	2.948	3.520[a]	2.948	3.090
PSS 0059+0003...	4.16	3.491	4.028	3.491	4.028	3.491	4.028
PC 0104+0215....	4.171	3.519	4.134[a]	3.519	4.134[a]	3.519	4.134[a]
BRI 0111−2819...	4.30	3.663	4.030	3.627	4.030	3.627	4.030
PC 0131+0120....	3.792	3.194	3.792[a]	3.194	3.792[a]	3.194	3.792[a]
Q0201+1120.......	3.61	3.047	3.610[a]	3.047	3.610[a]	3.047	3.227
						3.344	3.610[a]
PSS 0248+1802...	4.43	3.733	4.430[a]	3.733	4.430[a]	3.733	4.430[a]
Q0249−222..........	3.20	2.665	3.200[a]	2.665	3.200[a]	2.665	3.200[a]
PC 0345+0130....	3.638	3.060	3.638[a]	3.060	3.638[a]	3.060	3.638[a]
Q1500+0431.......	3.67	3.072	3.670[a]	3.072	3.670[a]	3.072	3.246
						3.353	3.670[a]
PC 1548+4637....	3.544	2.978	3.544[a]	2.978	3.090	2.978	3.011
PC 1640+4628....	3.700	3.123	3.700[a]	3.123	3.700[a]	3.674	3.700[a]
PC 2047+0123....	3.799	3.202	3.799[a]	3.202	3.799[a]	3.202	3.316
						3.486	3.799[a]
SGP 2050−359.....	3.49	2.921	3.490[a]	2.921	3.490[a]	2.921	3.490[a]
BR 2237−0607.....	4.558	3.840	4.558[a]	3.840	4.558[a]	3.840	4.558[a]
PC 2331+0216....	4.093	3.443	4.093[a]	3.443	4.093[a]	3.443	4.093[a]

[a] This redshift is within 5000 km s^{-1} of the z_{em}.

TABLE 7

Si IV Absorption Systems

Quasar (1)	z_{abs} (2)	$W_{rest}(1393)$ (Å) (3)	$W_{rest}(1402)$ (Å) (4)	DR (5)	Sample (6)	Note (7)
BR 0019−1522.....						
SGP 0046−293.....						
SGP 0057−274.....						
PSS 0059−0003....	3.5187	0.17	0.13	1.28	...	a
PC 0104+0215....	3.7081	0.52	0.39	1.34	M15, M30	
BRI 0111−2819...	3.8893	0.72	1.08	0.66	...	b
PC 0131+0120....	3.4228	0.52	0.24	2.17	M15	c
Q0201+1120.......	3.1984	0.63	0.30	2.14	M15, M30	
	3.3673	0.32	0.21	1.55	M15	
	3.3851	0.34	0.16	2.11	M15	
PSS 0248+1802...	3.9402	0.31	0.22	1.41	M15	
Q0249−222..........	2.6721	0.17	0.10	1.75	...	
PC 0345+0130....						
Q1500+0431.......	3.2261	0.56	0.47	1.19	M15, M30	
PC 1548+4637....						
PC 1640+4628....	3.6951	0.38	0.27	1.41	M15	
PC 2047+0123....	3.4961	0.21	0.40	0.53	...	b
	3.7254	0.36	0.27	1.35	M15	
	3.8153	0.14	0.12	1.23	...	d
SGP 2050−359.....	3.0930	0.32	0.25	1.29	M15	
	3.1711	0.42	0.28	1.51	M15	
BR 2237−0607.....	4.2460	0.08	0.07	1.28	...	
	4.2842	0.09	0.06	1.63	...	
	4.3596	0.52	0.27	2.00	M15	c
PC 2331+0216....						

[a] $|z(1548) - z(1551)| > 0.0015$, but other metal lines are found at the same redshift

[b] Doublet ratio is not appropriate, but other metal lines are found at the same redshift

[c] Two absorbers are combined, because they lie within 1000 km s^{-1} of each other

[d] Redshift of absorber is smaller than z_{min} or bigger than z_{max}

TABLE 8
DENSITY OF Si IV SYSTEMS

Criteria (1)	Sample (2)	Systems (3)	$\langle z_{abs} \rangle$[a] (4)	$\bar{z}$[b] (5)	$\bar{N}$[c] (6)	γ (7)	$\sigma(\gamma)$ (8)	G (9)	$\sigma(G)$ (10)
All included....................	M0	17[d]	...	...	...	0.30	3.22	−0.24	3.17
$W_0 > 0.15$, $\beta c > 5000$...	M15	12	3.524	3.660	$1.36^{+0.52}_{-0.39}$	−3.69	3.93	−4.23	4.00
$W_0 > 0.30$, $\beta c > 5000$...	M30	3	3.378	3.609	$0.29^{+0.28}_{-0.16}$	...	...	...	...
$W_0 > 0.60$, $\beta c > 5000$...	M60	0	...	3.597	<0.17	...	...	...	...

[a] Mean redshift of observed z_{abs}.
[b] Weighted mean redshift of the sample ranges in Table 6, following Tytler et al. 1987.
[c] Mean number of systems per unit redshift, at redshift $\bar{z}$.
[d] The system at $z = 2.6721$ in Q0249−222 is excluded.

5. SUMMARY AND DISCUSSION

We now discuss our main results and the differences from previous results:

1. We measure approximately twice the density of C IV systems with $W > 0.15$ Å that S90 measured. This could be a statistical accident.
2. Our samples are too small and lack the redshift range to measure the evolution of the number of C IV or Si IV absorbers.
3. When we combine our C IV samples with published samples to expand the redshift range, we see evolution at the 2–4 σ level, in the sense that was reported by S90. In either an Einstein–de Sitter ($\Lambda = 0$) or a flat universe ($\Lambda = 0.7$), the mean free path to intercept a C IV absorber increases with redshift.
4. The combined sample with $W > 0.15$ Å shows a shallower slope ($\gamma = -0.58 \pm 0.46$) than was reported by S90 ($\gamma = -1.26 \pm 0.56$). This difference is related to the first point and to our larger redshift range. The S90 data show little change in the $N(z)$ for $1.2 < z < 2.6$, followed by a marked drop off at higher z. We do not see this drop off, and we measure a density at $z \simeq 4$ that is not significantly lower than S90 measured at $z \simeq 2.4$.
5. We also see that the systems with C IV lines with $W > 0.3$ Å evolve much faster than the systems with weaker lines. S90 saw a hint of this.

Recently, spectra of 66 quasars at $z > 4$ were presented by Péroux et al. (2001). They produced a fairly large sample of metal absorption systems. They detected as many as 103 C IV absorption systems. The mean numbers of stronger C IV systems per unit redshift are roughly consistent with the previous results and our present result (M30 and M60). Our spectral resolution is approximately 2.5 times higher, which makes it much easier to identify weak lines.

Similar analyses have been presented for H I absorption lines. The DLA and Lyman limit system (LLS) features are easily detected. These previous results are summarized in Table 9 and Figure 10, which show the evolutionary trends of the number densities for various absorption systems. In Table 9, column (2) is the minimum rest-frame equivalent width. All detected lines must have equivalent widths larger than this limit. Column (3) shows the observed redshift ranges. Columns (4) and (5) refer to the indices, γ, in equation (3) and their errors. In column (6), G is the free parameter from equation (7), which is without an error, because we convert published values for an Einstein–de Sitter model to the $\Lambda = 0.7$ flat universe model. For high-ionized element like C IV and Si IV, the number density evolutions show decreasing trends with redshift at $z \geq 2$. On the other hand, those of H I absorbers and low-ionized element show opposite trends at lower and similar redshifts. Figure 10 shows the evolutionary trends. For comparison, we plot the number density evolution with $G = 0$ and $N_0 = 1.0$. Here we must note that this figure shows only the rough evolutionary trends. The differences in the minimum equivalent widths prevent ready comparison of the absolute number densities. However, it is clear that the evolutionary trends are not the same for all ions.

We have not explored the physical explanations for these trends, which presumably involve a combination of structure formation, chemical evolution and ionization changes.

About the structure of C IV absorbers, Petitjean & Bergeron (1994) reported that there is a strong correlation between the total W of a C IV system and its number of

TABLE 9
EVOLUTIONS OF NUMBER DENSITIES FOR VARIOUS ABSORPTION LINES

Element (1)	W_{min} (Å) (2)	Redshift Range (3)	γ (4)	$\sigma(\gamma)$ (5)	G (6)	Reference (7)
C IV	0.15	2.3–4.5	−1.88	1.91	−2.45	1
	0.15	1.2–3.7	−1.26	0.56	−1.88	2
Si IV.........	0.15	2.7–4.6	−3.69	3.93	−4.23	1
Mg II	0.60	0.25–2.3	1.11	0.46	0.31	3
DLA	10	0.008–3.5	1.15	0.55	0.45	4
LLS.........	($\tau \geq 1$)	0.32–4.11	1.50	0.39	0.88	5

REFERENCES.—(1) This study; (2) Steidel 1990; (3) Aldcroft et al. 1994; (4) Lanzetta et al. 1995; (5) Stengler-Larrea et al. 1995.

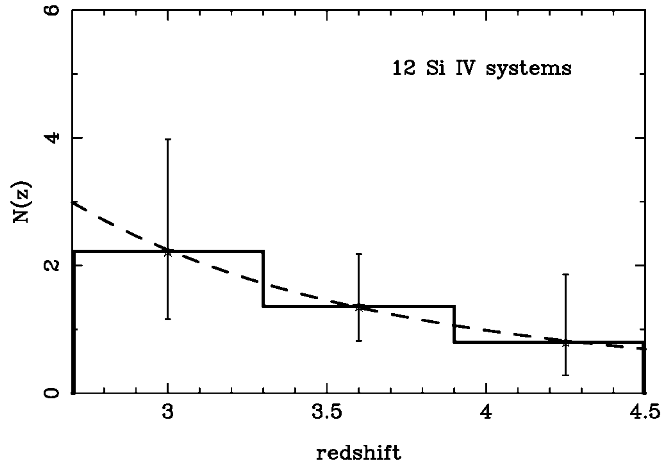

FIG. 9.—Same as Fig. 3, but for sample M15 of the Si IV systems. The dashed curve is the result of a maximum likelihood estimation for eq. (7) with $G = -4.23$.

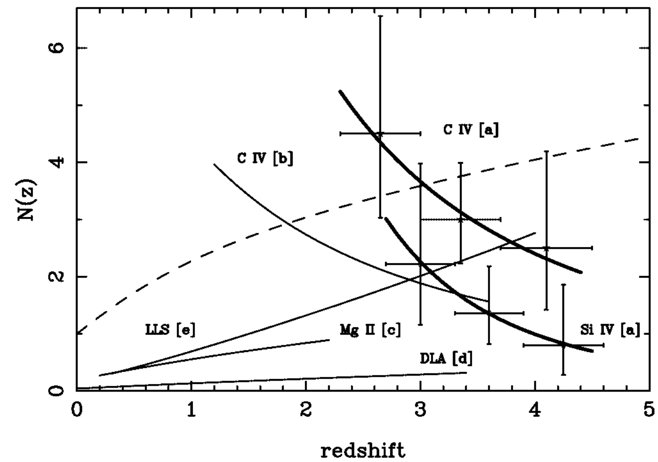

FIG. 10.—Evolution of the number densities of various absorption lines following eq. (7). For comparison, the dashed line represents the evolution with $G = 0$ and $N_0 = 1.0$. (*a*) This study; (*b*) Steidel 1990; (*c*) Aldcroft, Bechtold, & Elvis 1994; (*d*) Lanzetta, Wolfe, & Turnshek 1995; (*e*) Stengler-Larrea et al. 1995.

velocity components. It is also suggested that the highly ionized ions such as C IV and Si IV are produced in the low-density regions which cover the high-density regions producing low-ionization Mg II and H I absorption lines. This structure was guessed from the differences between the absorption-line profiles for high- and low-ionization absorption lines (Lu, Sargent, & Barlow 1996). The faster evolution of the C IV systems with larger *W*-values then implies that there are more components at lower redshifts. This may be related to structure formation, as small galaxies merge into larger galaxies.

Steidel found that the evolution of the doublet ratio of C IV absorbers could not be explained if column density does not evolve. Therefore, he concluded that the evolution of number density of C IV absorbers is mainly affected by a systematic change in the abundance of carbon in the gas (S90). But Songaila (2001) found that the carbon metallicity is $Z = 5 \times 10^{-4}$ at $z = 4$ and does not change dramatically toward lower redshift. The evolution of the C IV abundance is still unclear.

We would like to thank N. Kashikawa and K. Kawabata for their advice and to K. Denda, K. Ohkoshi, and T. Yamamoto for their comments. D. T. is grateful for the hospitality of the National Astronomical Observatory of Japan in Mitaka, where this work was begun during a visit in 1999 that was sponsored by the Ministery of Education, Science, Sports, and Culture. D. T. was supported in part by NSF grant AST 99-00842, and NASA grant NAG 5-9224. L. S. L. was supported by a University of California President's Postdoctoral Fellowship. A. M. W. was supported in part by NSF grant AST 00-71257. We wish to thank an anonymous referee for their concise report.

REFERENCES

Aldcroft, T. L., Bechtold, J., & Elvis, M. 1994, ApJS, 93, 1
Bergeron, J., & Boissé, P. 1991, A&A, 243, 344
Chen, H.-W., Lanzetta, K. M., & Webb, J. K. 2001, ApJ, 556, 158
Foltz, C. B., Weymann, R. J., Peterson, B. M., Sun, L., Malkan, M. A., & Chaffee, F. H., Jr. 1986, ApJ, 307, 504
Lanzetta, K. M., Wolfe, A. M., & Turnshek, D. A. 1995, ApJ, 440, 435
Lu, L., Sargent, W. L. W., & Barlow, T. A. 1996, ApJS, 107, 475
Oke, J. B., et al. 1995, PASP, 107, 375
Péroux, C., Storrie-Lombardi, L. J., McMahon, R. G., Irwin, M., & Hook, I. M. 2001, AJ, 121, 1799
Petitjean, P., & Bergeron, J. 1994, A&A, 283, 759
Sargent, W. L. W., Boksenberg, A., & Steidel, S. S. 1988, ApJS, 68, 539 (SBS88)
Songaila, A. 2001, ApJ, 561, L153
Steidel, S. S. 1990, ApJS, 72, 1 (S90)
Stengler-Larrea, E. A., et al. 1995, ApJ, 444, 64
Storrie-Lombardi, L. J., & Wolfe, A. M. 2000, ApJ, 543, 552
Tytler, D. 1981, Nature, 291, 289
Tytler, D., Boksenberg, A., Sargent, W. L. W., Young, P., & Kunth, D. 1987, ApJS, 64, 667
Young, P. J., Sargent, W. L. W., & Boksenberg, A. 1982, ApJS, 48, 455
Young, P. J., Sargent, W. L. W., Boksenberg, A., Carswell, R. F., & Whelan, J. A. J. 1979, ApJ, 229, 891